HHS Public Access

Author manuscript

Nature. Author manuscript; available in PMC 2016 May 03.

Published in final edited form as:

Nature. 2015 June 11; 522(7555): 173–178. doi:10.1038/nature14484.

Cloning and Variation of Ground State Intestinal Stem Cells

Xia Wang[1,10], **Yusuke Yamamoto**[1,10], **Lane H. Wilson**[1,2], **Ting Zhang**[3], **Brooke Howitt**[4], **Melissa A. Farrow**[5], **Florian Kern**[3], **Gang Ning**[1], **Yue Hong**[1], **Chiea Chuen Khor**[3], **Benoit Chevalier**[1], **Denis Bertrand**[3], **Lingyan Wu**[3], **Niranjan Nagarajan**[3], **Francisco A. Sylvester**[6], **Jeffrey S. Hyams**[6], **Thomas Devers**[7], **Roderick Bronson**[8], **D. Borden Lacy**[5], **Khek Yu Ho**[9], **Christopher P. Crum**[4], **Frank McKeon**[1,3,9,10,*], and **Wa Xian**[1,2,4,*]

[1]The Jackson Laboratory for Genomic Medicine, Farmington, CT, USA

[2]Department of Genetics and Developmental Biology, University of Connecticut Health Center, Farmington, CT, USA

[3]Genome Institute of Singapore, A-STAR, Singapore

[4]Department of Pathology, Brigham and Women's Hospital, Boston, MA USA

[5]Department of Pathology, Microbiology, and Immunology, Vanderbilt University School of Medicine, Nashville, TN, USA

[6]Division of Gastroenterology, Connecticut Children's Medical Center, Hartford, CT, USA

[7]Department of Medicine, University of Connecticut Health Center, Farmington, CT, USA

[8]Department of Microbiology and Immunobiology, Harvard Medical School, Boston, MA, USA

[9]Department of Medicine, National University Health System, Singapore

[10]Multiclonal Therapeutics, Inc., Farmington, CT, USA

Summary

Stem cells of the gastrointestinal tract, pancreas, liver, and other columnar epithelia collectively resist cloning in their elemental states. Here we demonstrate the cloning and propagation of highly clonogenic, "ground state" stem cells of the human intestine and colon. We show that derived stem cell pedigrees sustain limited copy number and sequence variation despite extensive serial passaging and display exquisitely precise, cell-autonomous commitment to epithelial differentiation consistent with their origins along the intestinal tract. This developmentally patterned and epigenetically maintained commitment of stem cells likely enforces the functional specificity of the adult intestinal tract. Using clonally-derived colonic epithelia, we show that

*Correspondence to: Wa Xian, Xianmckeon2014@gmail.com, 1-860-480-1188. Frank McKeon, 1-860-480-1263.

[11]these authors contributed equally to this work.

Author Contributions

Experimental design and conception were done by WX, FM, DBL, HKY, and CPC. XW cloned and differentiated the intestinal stem cells with help from LHW, FK, GN, YH. YY and XW prepared the genomic and gene expression analyses together with FK, GN, CCK, and YY, TZ, DB, and NN performed all computational and bioinformatics work. BH and CPC obtained fetal tissues and FAS, JSH, and TD provided endoscopic biopsies, and RB analyzed the xenografts. The *C. difficile* experiments were designed and executed by BC, LHW, MAF, and DBL. WX and FM wrote the manuscript with input from all others.

toxins A or B of the enteric pathogen *C. difficile* recapitulate the salient features of pseudomembranous colitis. The stability of the epigenetic commitment programs of these stem cells, coupled with their unlimited replicative expansion and maintained clonogenicity, suggests certain advantages for their use in disease modeling and regenerative medicine.

Introduction

While dominating prospective strategies for regenerative medicine, embryonic stem cells (ESC) and induced pluripotent stem cells (iPSC) face formidable challenges including risk of teratoma, complex guiding protocols for lineage specificity, and limited regenerative capacity of the lineages ultimately produced[3–8]. The success and promise of iPSCs have largely overshadowed efforts to harness stem cells intrinsic to regenerative tissues. Green and colleagues developed methods for cloning epidermal stem cells[9] that form a stratified epithelium upon engraftment, and these methods have been successfully applied to corneal, thymic, and airway epithelia[10–12]. However, stem cells of columnar epithelial tissues resist cloning in a manner that maintains their immaturity during proliferative expansion, and instead must be carried forward as regenerative, differentiating "organoids"[13–18]. Despite their obvious potential in regenerative medicine and constant improvement[19], the very low percentage of clonogenic cells in organoids limits the kinetics of their propagation as well as their utility for exploring the elemental stem cell.

The present study reports the cloning and propagation of "ground state" human intestinal stem cells (ISC^{GS}). This technology offers insights into the molecular and functional features of columnar epithelial stem cells and their utility for disease modeling and regenerative medicine.

Cloning human fetal intestinal stem cells

We developed media (herein SCM-6F8) containing novel combinations of growth factors and regulators of TGF-β/BMI1, Wnt/β-catenin, EGF, IGF, and Notch pathways[9,20–21] that supports the maintenance of human intestinal stem cells in a highly clonogenic, ground state form. Thus single cell suspensions of intestinal epithelia derived from 20- to 22-week-old fetal demise cases yield colonies comprised of highly immature cells in which differentiation markers can be induced by Notch suppression (Fig. 1a). Following induced differentiation via Wnt withdrawal, we were unable to recover ground state stem cells by our methods (Extended Data Fig. 1).

The clonogenicity of cells in the colonies was determined by single cell transfer to be greater than 50% (Fig. 1b). This high clonogenicity permits the rapid generation of single cell "pedigree" lines for expansion and characterization of lineage fates upon differentiation[12] (Fig. 1b). Pedigree lines of ISC^{GS} and tracheobronchial stem cells (TBSC^{GS})[12] grown for several months in culture were differentiated in air-liquid interface (ALI) cultures for 10–30 days (Fig. 1c). The ISC^{GS} formed a highly uniform, 3-D serpentine pattern, whereas TBSC^{GS} produced a stratified epithelium with apically positioned ciliated and goblet cells. Histological sections of differentiated ICS^{GS} revealed a columnar epithelium of villus-like structures marked by goblet (Muc2+), endocrine (chromogranin A+), and Paneth cells and

polarized villin expression (Fig. 1d; Extended Data Fig. 1d), indicating the progeny of a single ISC^{GS} can give rise to all epithelial lineages typically found in the small intestine. Importantly, differentiation of these ground state stem cells is accomplished by exposure to an air-liquid interface rather than a removal of factors such as Wnt that maintain immaturity.

While principal component analysis (PCA) of differentially expressed genes of ground state stem cells and ALI differentiated tissue showed great divergence as expected for columnar and stratified epithelia, the gene expression profiles of undifferentiated ISC^{GS} and TBSC^{GS} differed by less than 4% (>2.0-fold, $p<0.05$) (Fig. 1e). ISC^{GS} showed high expression of intestinal stem cell markers such as OLFM4, CD133[22], Lgr5[23], and Lrig1[24], whereas those from the airways had the typical stem cells markers of stratified epithelia (Krt14, Krt5, and Tp63[11]) (Fig. 1f).

Intestinal stem cell variation

Approximately one in 2,000 cells from duodenum (I^{du}SC), jejunum (I^{je}SC), and ileum (I^{il}SC) of a 21-week old fetal intestine form a colony (Fig. 2a). Although these colonies were morphologically indistinguishable in culture, whole genome expression analysis of multiple pedigrees showed a consistent, region-specific signature of 24–178 genes (>1.5-fold, $p<0.05$; Fig. 2b; Extended Data Fig. 2).

After 10 days at an ALI, I^{du}SC and I^{je}SC gave rise to a finer pattern of epithelial folds than that produced by I^{il}SC (Fig. 2c). By histology, villi appear progressively more robust along the anterior-posterior axis, with I^{il}SC producing the larger villi and more numerous goblet cells (Fig. 2d,e). Interestingly, the epithelia derived from I^{du}SC expressed markers more typical of gastric epithelium (e.g. TFF2 and Muc5AC) consistent duodenum's location between the stomach and the small intestine (Extended Data Fig. 2a,b,c). I^{je}SC-derived epithelium, however, expressed Muc2 consistent with intestinal epithelium (Extended Data Fig. 2c), and I^{il}SC produced an epithelium more akin to colon (Fig. 2f). The pattern of proliferation in the ALI epithelia as measured by Ki67 staining was generally confined to cells proximal to the support membrane (Fig. 2e,f). PCA mapping of gene expression revealed more divergence among ALI-differentiated tissue than among the intestinal stem cells (Fig. 2g).

Colon stem cells

We also generated single cell pedigree lines from the ascending, transverse, and descending colon from the same 21-week fetal demise case (Fig. 3a). The variation in gene expression between the stem cells of these colonic segments was minimal with signatures of 19–28 genes (>1.5-fold, $p<0.05$; Fig. 3b). As with pedigrees derived from the intestinal epithelium, those from the colon could be propagated for months without loss of clonogenicity (not shown). Differentiation of these colon pedigrees under identical ALI conditions employed for the intestinal stem cells resulted in networks of 3-D, large-diameter structures (Fig. 3c). Consistently, the histology of these ALI cultures revealed patterns of broad intestinal glands dominated by goblet cells (Fig. 3d). These ALI-generated tissues showed strong staining for intestinal goblet cell marker Muc2, as well as polarized villin and Krt20 typical of

differentiated colonic epithelium (Fig. 3e). And while the colonic stem cells as a group showed minor differences in gene expression (cf. Fig. 3b), they gave rise to epithelia with more distinct gene expression profiles (Extended Data Fig. 3). PCA mapping of these expression data showed a clustering of the colon stem cells relative to the intestinal stem cells with increasingly distant spaces occupied by stem cells of the ileum, jejunum, and duodenum, respectively (Fig. 3f). This distinction in global gene expression patterns is reflected, for instance, in the differential expression of transcription factors. In particular, Onecut2, NROB2, TRPS1, and ZNF503 show relatively high expression in the small intestine stem cells, whereas those of the colon showed a bias for Hox genes as well as the global chromatin organizer genes SATB1 and SATB2 (Fig. 3g,h).

Columnar versus stratified epithelia

The expression profiles of stem cells of human intestinal tract enabled a detailed comparison with those of stratified epithelia including human epidermis, corneal epithelium, mammary gland, prostate gland, and upper airway. From this analysis it is clear that stratified epithelia, all of which depend on the p53-related stem cell marker p63 for long-term self-renewal[11], occupy a distinct expression space from that of the intestinal stem cells or other columnar epithelial stem cells (Fig. 4a). A survey of genes whose expression is associated with stem cells of one of these two major classes of epithelia revealed a strong bias for Olfm4, CD133[22], Lgr5[23], Nr5a2[25], Id2, Lrig1[24], EphB2, Ascl2, and EphB3 in the intestinal stem cells, while the stratified epithelial stem cells expressed Znf750, Tp63, and Krt5 (Fig. 4b). Many of the markers differentially appearing in the intestinal stem cells, such as Olfm4, Lgr5, and Ascl2, are not general columnar epithelial stem cell markers as evidenced by their absence in fallopian tube stem cells, though Lrig1 is more highly expressed in fallopian tube stem cells than either those of the intestine or the colon (Extended Data Fig. 4a). Notably, Bmi1, a member of the Polycomb group (PcG) PRC1-like complex implicated in self-renewal in both hematopoietic[26] and as reserve cells for proliferating, Lgr5+ intestinal stem cells[27–29], was not differentially expressed in the cloned intestinal versus stratified epithelial stem cells. And while many of the typical markers of intestinal stem cells such as Lgr5, CD44, Lrig1, EphB2, and ASCL2 show a decrease in expression as the intestinal stem cells are differentiated in ALI cultures, Bmi1 did not (Extended Data Fig. 4b,c). These findings suggest that we are cloning either crypt cells or so-called “+4” cells that have become crypt-like in their expression patterns. We also examined transcription factors differentially expressed in ISC compared to stratified epithelial stem cells in an effort to understand the regiospecificity of commitment programs of stem cells along the intestinal tract (Fig. 4c). In addition to six transcription factors that were uniformly highly expressed in stem cells of the intestinal tract (CREB3L1, Myb, NR5A2, IRF8, HNF4G, and Msx2) versus tracheobronchial stem cells, this analysis revealed limited sets of transcription factors differentially expressed in stem cells along the anterior-posterior axis of the intestinal tract that conceivably function in maintaining commitment states. For instance and consistent with previous observations[30], GATA4 and GATA6 were expressed most strongly in the anterior portions of the intestinal tract (Fig. 4c). Significantly, the selective deletion of GATA4 and GATA6 in the murine duodenum and jejunum results promotes ileal properties and a detrimental phenotype[30,31], suggesting a role for these transcription factors in

maintaining segmental identity acting at the level of the stem cell. Similarly, the requirement for Onecut2 in the duodenum[32] might be at the level of the duodenal stem cells. It is likely that analyses of cloned stem cells from the various segments of the intestinal tract will help to unravel the roles of such segment-specific transcription factors in the establishment of commitment and differentiation programs. Importantly, the overall properties of ISCs from fetal sources are conserved in those derived from endoscopic biopsies of pediatric and adult cases (Fig. 4d,e,f).

Genomic and lineage stability

Human ESC and iPSC lines acquire with successive passages genomic structural variations including some that confer a selective advantage[33,34]. To assess the genomic stability of our ISC^{GS}, we examined copy number (CNV) and single nucleotide variation (SNV) in two independent ISC^{GS} pedigrees derived from the ileum of one fetal demise case after 50 (passage 5; P5), 100 (P10), 150 (P15), and 200 days (P20) of continuous proliferation (Fig. 5a,b). At P5, when single ISC^{GS} pedigrees can be amplified to an estimated 300 million to 75 billion cells, no chromosomal aneuploidies were detected, though one pedigree showed three interstitial deletions affecting two genes (Fig. 5c; Extended Data Fig. 5a; SI Table 1). This low level of structural variation was maintained though passage 10 though increased by P15 and at P20 one of the pedigrees showed a frank trisomy of chromosome 12 (Fig. 5c; Extended Data Fig. 5a; SI Table 1). A similar upward trend in CNV as a function of passage number was observed in five intestinal pedigrees (pedigrees 3–7) derived from a separate fetal demise case (Extended Data Figs. 5, 6; SI Tables 1, 2).

By exome sequencing, our original two pedigrees showed few (0–1) non-synonymous mutations through passage 10, and these increased modestly (1–2 new non-synonymous mutations) through P15 and P20 (Extended Data Fig. 5a). None of these non-synonymous mutations have been reported as driver genes in human cancers. A similar trend was observed in the five pedigrees from the second fetal demise case followed through P5 and P25. By P25 the range of non-synonymous SNVs increased to 2–10 per clone, and while not involving obvious cancer driver genes, did include genes such as Ect2L and EP300 that might provide a selective growth advantage (Extended Data Fig. 5c). These data indicate that most pedigrees sustain few genomic changes within the first 100 days of proliferative expansion. By P15 and through P25, however, half the pedigrees showed evidence for aneuploidy as well as an increase in interstitial CNV and SNVs with allele frequencies nearing 0.5, suggesting the rise of an advantaged subclone. We asked how these late passage genomic changes might impact differentiation by comparing early and late passages of pedigree 2 in ALI differentiation. By all histological criteria, including Alcian blue staining for goblet cells and intestinal marker staining, we could not distinguish the ALI differentiated epithelia derived from P7, P17, and p27 (Fig. 5d; Extended Data Fig. 7). Similarly, we note that these intestinal stem cell pedigrees do not lose (or gain) clonogenicity when tested at P7 and p16, which remain stably above 50% (Fig. 5e,f). Lastly, we found no evidence of tumorigenicity by these ground state intestinal stem cells, including those at P25 harboring aneuploidies, following their subcutaneous implantation to immunodeficient (NOD.Cg-Prkdc^{scid} Il2rg^{tm1Wjl}/SzJ) mice[35] (Extended Data Fig. 8).

Modeling *C. difficile* infections

Clostridium difficile (Cd) is a gram-positive, spore-forming bacterium and the primary cause of nosocomial diarrhea and pseudomembranous colitis[36]. The pathogenicity of Cd is linked to its production of two similar, high molecular weight toxins TcdA and TcdB. While together TcdA and TcdB cause fluid secretion, inflammation, and colonic tissue damage, their respective and possible synergistic roles have been difficult to ascertain[37–39]. We therefore challenged colonic epithelia derived from cloned, ground state colonic stem cells with recombinant TcdB (Fig. 6a,b; Extended Data Fig. 9a,b). At higher concentrations or longer time points there is a loss of goblet cells, disruption of the crypt architecture, cell polarity, and a specific loss of tight versus adherens junction proteins that correlates with increased dextran permeability (Fig. 6c). These dose-response changes in the ALI colonic epithelium mirror those of *C. difficile*-associated pseudomembranous colitis (Fig. 6d, Extended Data Fig. 9a,b). Microarray analysis of ALI-generated colonic epithelia following nine TcdB treatment conditions revealed alterations in gene expression in a time- and dose-dependent manner (Fig. 6e,f; Extended Data Fig. 9c–f). Pathway analysis indicated that TcdB triggers changes in gene expression related to inflammation, RhoB-mediated actin regulation, and junctional dynamics previously implicated in *C. difficile* pathology[40,41]. In addition, this analysis revealed that DUOX2 and DUOXA2 were consistently the two highest up-regulated genes (Fig. 6e,f). These proteins form an enzyme capable of producing hydrogen peroxide and have been implicated in the inflammation of inflammatory bowel disease (IBD)[42]. Finally, we also tested *C. difficile* TcdA in our model. TcdA is reported to be a specific enterotoxin[36,37], and indeed we found that it triggers similar cytopathic and permeability changes in ALI models of human colonic epithelium (Extended Data Fig. 10), albeit at lower doses than those effective for TcdB. Together these findings underscore the potential of this model system to recapitulate and elucidate *C. difficile* pathology.

Discussion

Adult stem cells of the highly regenerative intestinal tract remain largely defined by metabolic, marker profiling, or lineage tracing experiments *in vivo* or transplantation of cells from intestinal organoids[23, 43–44]. As stem cells comprise only minor component of organoids- perhaps less than 1%[45], the molecular features of stem cells of columnar epithelia such as the intestinal tract have remained unclear. Therefore the selective cloning and proliferative expansion of highly clonogenic, ground state intestinal stem cells described here offers a first glimpse into the molecular properties of these cells. Our inability to convert differentiated cells to clonogenic cells supports the notion that we are cloning resident stem cells rather than somehow “reprograming” differentiated enterocytes. These resident stem cells possess robust epigenetic programs of commitment to regiospecific intestinal differentiation that are stable despite more than six months of continuous propagation. This cell-autonomous regiospecificity of stem cells along the intestinal tract argues against a unitary “intestinal stem cell” or even one each for the histologically recognized segments but rather a developmentally established spectrum of stem cells that ultimately maintains the histological and functional properties that define these segments. An heuristic deciphering of the commitment code from the regiospecific expression patterns presented here will guide parallel efforts with iPSCs to achieve appropriate lineage fates[46].

Interestingly, many inductive signaling pathways and transcription factors implicated in embryonic gut formation[47] may act to reinforce commitment codes via continued expression in stem cells of the intestinal tract.

We anticipate that the ability to maintain these stem cells in their elemental state will enable the discovery of epigenetic mechanisms that underlie properties of very long-term self-renewal, exquisitely precise lineage commitment, and the intrinsically directed, self-assembly of differentiated epithelia. Though we demonstrate the potential of clonally-derived colonic epithelia to model the pathogenesis of *C. difficile* toxins, we anticipate the need to restore complexity in the form of mesenchyme, immune cells, enteric neurons, and perhaps components of the microbiome[48] to fully recapitulate disease dynamics. In particular, enteric maladies such as inflammatory bowel disease represent significant medical challenges whose etiologies most likely reside in interactions between the immune system, intestinal mucosa, and intestinal flora[49,50]. Finally, the ability to clone patient-specific, ground state stem cells from endoscopic biopsies, coupled with their orders-of-magnitude expansion kinetics over organoids, favors their use in regenerative medicine, pre-clinical trials, and disease modeling.

Methods

In vitro culture of human small intestinal and colonic epithelial stem cells

Intestinal tissue from 20- to 21-week-old late fetal demise cases were obtained under parent consent as de-identified material under approved institutional review board protocols at the Brigham and Women's Hospital, Boston, MA, USA (2009P002281). Terminal ileum endoscopic biopsies were obtained under informed consent and institutional review board approval at the Connecticut Children's Medical Center, Hartford, CT USA (15-047J-2). Fetal intestinal tissue or 1 mm endoscopic biopsies from terminal ileum were collected into cold F12 media (Gibco, USA) with 5% fetal bovine serum (HyClone, USA) and then minced by sterile scalpel into 0.2–0.5 mm^3 sizes to a viscous and homogeneous appearance. The minced tissue was digested in 2 mg/ml collagenase type IV (Gibco, USA) at 37°C for 30–60 min with agitation. Dissociated cells were passed through a 70 μm Nylon mesh (Falcon, USA) to remove aggregates and then were washed four times in cold F12 media, and then seeded onto a feeder layer of lethally irradiated 3T3-J2 cells[9,12] in c-FAD media[9] modified to SCM-6F8 media by the addition of 125 ng/mL R-spondin1 (R&D systems, USA), 1 μM Jagged-1 (AnaSpec Inc, USA), 100 ng/ml human Noggin (Peprotech, USA), 2.5 μM Rock-inhibitor (Calbiochem, USA), 2 μM SB431542 (Cayman chemical, USA), and 10 mM nicotinamide (Sigma-Aldrich, USA). Cells were cultured at 37°C in a 7.5% CO_2 incubator. The culture media was replaced every two days. Colonies were digested by 0.25 % trypsin-EDTA solution (Gibco, USA) for 5–8 min and passaged every 7 to 10 days. Colonies were trypsinized by TrypLE Express solution (Gibco, USA) for 8–15 min at 37°C and cell suspensions were passed through 30 μm filters (Miltenyi Biotec, Germany). Approximately 20,000 epithelial cells were seeded to each well of 6-well plate. Cloning cylinder (Pyrex, USA) and high vacuum grease (Dow Corning, USA) were used to select single colonies for pedigrees. Gene expression analyses were performed on cells derived from passage 4–8 (P4–P8) cultures.

Histology and Immunostaining

Histology, hematoxylin and eosin (H&E), Alcian blue, Periodic acid–Schiff (PAS), Rhodamine B staining, immunohistochemistry, and immunofluorescence were performed using standard techniques. For immunofluorescence and immunohistochemistry, 4% paraformaldehyde-fixed, paraffin embedded tissue sections were subjected to antigen retrieval in citrate buffer (pH 6.0, Sigma-Aldrich, USA) at 120 °C for 20 min, and a blocking procedure was performed with 5% bovine serum albumin (BSA, Sigma-Aldrich, USA) and 0.05 % Triton X-100 (Sigma-Aldrich, USA) in phosphate-buffered saline (PBS; Gibco, USA) at room temperature for 1 hr. Primary antibodies used in this study and staining condition were listed in Supplementary Information Table 3. All images were captured by using the Inverted Eclipse Ti-Series (Nikon, Japan) microscope with Lumencor SOLA light engine and Andor Technology Clara Interline CCD camera and NIS-Elements Advanced Research v.4.13 software (Nikon, Japan) or LSM 780 confocal microscope (Carl Zeiss, Germany) with LSM software. Bright field cell culture images were obtained on an Eclipse TS100 microscope (Nikon, Japan) with Digital Sight DSFi1camera (Nikon, Japan) and NIS-Elements F3.0 software (Nikon, Japan).

Stem cell differentiation

Air-liquid interface (ALI) culture of intestinal and colonic epithelial cells was performed as described[12,51]. Briefly, *Transwell* inserts (Corning, USA) were coated with 20% Matrigel (BD Biosciences, USA) and incubated at 37 °C for 30 min to polymerize. 200,000 irradiated 3T3-J2 cells were seeded to each transwell insert and incubated at 37 °C, 7.5% CO_2 incubator overnight. QuadroMACS Starting Kit (LS) (Miltenyi Biotec, Germany) was used to purify the stem cells by removal of feeder cells. 200,000–300,000 stem cells were seeded into each *Transwell* insert and cultured with SCM-6F8. At confluency (3–7 days), the apical media was removed through careful pipetting and the cultures were continued for an additional 6–12 days before analysis.

Clostridium difficile toxin treatment and epithelial permeability assay

Clostridium difficile toxins A and B (TcdA, TcdB) were prepared as described[52]. Intestinal stem cells were differentiated in air-liquid interface cultures as described above and treated with 100, 250, 500 pM and 10 nM TcdA or TcdB for 0, 8, 16, and 24 hr). At these time points, membranes with differentiated epithelia were collected for histology and microarray analysis. 4kDa FITC-dextran (Sigma-Aldrich, USA) was added to the apical chamber of the *Transwell* chambers for a final concentration of 0.5 mg/ml. Media was removed from the bottom compartment after different incubation times and fluorescence was read by fluorometer (Infinite® M1000 PRO, excitation 490 nm, emission 520 nm, Tecan, USA).

Implantation of intestinal stem cells

Intestinal stem cells (1.5 million cells) from different pedigrees with 50 % of Matrigel (BD Bioscience, USA) were subcutaneously implanted into female, six-eight-week-old immunodeficient (NOD.Cg-Prkdc^{scid} Il2rg^{tm1Wjl}/SzJ) mice[35] under IACUC approval (100533-1115) To test spontaneous transformation of the stem cells, mice were monitored every month (up to 4 months).

RNA and genomic DNA sample preparation

For stem cell colonies, RNA was isolated using PicoPure RNA Isolation Kit (Life Technologies, USA). For ALI-differentiated epithelia, RNA was isolated using Trizol RNA Isolation Kit (Life Technologies, USA). RNA quality (RNA integrity number, RIN) was measured by analysis Agilent 2100 Bioanalyzer and Agilent RNA 6000 Nano Kit (Agilent Technologies, USA). RNAs having a RIN > 8 were used for microarray analysis. Genomic DNA was extracted with DNeasy Blood & Tissue kit (Qiagen, Netherlands) from intestinal and colonic stem cells for CNV analysis and exome capture sequencing. For genomic DNA extraction, human intestinal and colonic stem cells were isolated from mouse 3T3 feeder layer using QuadroMACS Starting Kit (Miltenyi Biotec, Germany). Genomic DNA concentration was measured with Qubit® dsDNA BR Assay Kit (Life Technologies, USA).

Expression microarray and bioinformatics

Total RNAs obtained from immature colonies and ALI differentiated structure were used for microarray preparation with WT Pico RNA Amplification System V2 for amplification of DNA and Encore Biotin Module for fragmentation and biotin labeling (NuGEN Technologies, USA). RNA quality (RNA integrity number, RIN) was measured by analysis using an Agilent 2100 Bioanalyzer and Agilent RNA 6000 Nano Kit (Agilent Technologies, USA). RNAs having a RIN > 8 were used for microarray analysis. All samples were prepared according to manufacturer's instructions and hybridized onto GeneChip Human Exon 1.0 ST Array (Affymetrix, USA). GeneChip operating software was used to process all the Cel files and calculate probe intensity values. To validate sample quality, quality checks were conducted using Affymetrix Expression Console software. The intensity values were log2-transformed and imported into the Partek Genomics Suite 6.6 (Partek Incorporated, USA). Exons were summarized to genes and a 1-way ANOVA was performed to identify differentially expressed genes. For two sample statistics, p-values were calculated by student t-test for each analysis. Unsupervised clustering and heatmap generation were performed with sorted datasets by Euclidean distance based on average linkage clustering, and Principal Component Analysis (PCA) map was conducted using all or selected probe sets by Partek Genomics Suite 6.6. Gene Set Enrichment Analysis (GSEA)[53] was performed for C. diff toxin B treatment. For the region-specific gene signature of small intestine and colon comparison (PD, PJ and MI for Figure 2b and AC, TC and DC for Figure 3b), differentially-expressed genes were selected with a cutoff value of 1.5 fold and $p < 0.05$ in each comparison (e.g. 1) PD vs. PJ and 2) PD vs. MI) and then intersected genes in 2 gene lists of each comparison were taken as regio-specific gene sets. In the heatmaps (Fig. 2b and 3b), 3 regio-specific gene sets (PD, PJ and MI, or AC, TC and DC) were combined, and the heatmaps were made with Euclidean distance based on average linkage clustering. For *C. difficile* toxin B treatment data sets, samples from indicated time points and dosages were compared with control (untreated samples). Differentially-expressed genes (2-fold up-regulated and down-regulated genes) were counted and plotted in 3D column plots (Extended Data Figure 8c). In comparison of 500 pM 24 hrs toxin B treatment with control, 39 genes were significantly upregulated (cutoff value: 3 fold and $p < 0.05$) and a heatmap (Figure 6e) was made with 39 genes using all samples. The whole genome expression data of 500 pM 24 hrs toxin B treatment vs. control were applied to GSEA program to detect significantly enriched pathway in toxin B treatment. Selected pathways (from KEGG) were

shown in Figure 6d. Datasets generated for this study have been submitted to the National Center for Biotechnology Information Gene Expression Omnibus (GEO) database under files GSE57584 and GSE63880.

Copy number variation

For copy number variation analysis of stem cell pedigrees and passage 0 pooled sample, genomic DNA samples were genotyped with HumanOmniExpress BeadChip Kit for clone 1 and 2 (passage 5, 10, 15 and 20) (Illumina, USA) and Illumina HumanOmniZhonghua BeadChip Kit for clones 3 to 7(passage 5 and 25) following the manufacturer's instructions. Analysis of BeadChip was performed using GenomeStudio Software (Illumina, USA). Illumina high-density SNP genotyping data was converted to kilobase-resolution detection of copy number variation. CNV detected in passage 0 pooled samples are considered as germline CNVs and removed in the analysis. The data was generated by PennCNV[54]. Genes within 10Kb of CNV regions are reported. The parameter is set as "-expandleft 10k" and "-expandright 10k". Other parameters are default. Confidence score > 10 was used as a cutoff. The call rates for CNV were all greater than 99%, and two larger CNV amplification and deletion events were validated by quantitative PCR.

Exome capture sequencing

For Exome capture and high-throughput sequencing for intestinal stem cells (pedigree 1 and 2), 50 ng of gDNA was used to perform Nextera Expanded Exome Kit (Illumina, USA). For pedigree 3 to 7, 1μg of genomic DNA was sheared using a Covaris S1 Ultrasonicator (Covaris, USA), end-repaired, A-tailed, and Adaptor-ligated. Exome capture was performed using a Tru-seq Exome Enrichment Kit (Illumina, USA) following the manufacturer's instructions. Multiplexed libraries were sequenced on an Illumina HiSeq sequencer using 101-bp paired-end reads. Reads were aligned to the reference genome (UCSC hg19) using Burrows Wheeler Aligner (BWA, 0.6.2)[55]. PCR duplicates were removed using PICARD-1.94 (http://picard.sourceforge.net). The Genome Analysis Toolkit (GATK framework version 2.6.4)[56] was used to realign reads near indels and to recalibrate base quality values.

When running GATK, the minimum phred-scaled confidence threshold at which variants were called (-stand_call_conf) was 50, and the minimum phred-scaled confidence threshold at which variants were emitted (-stand_emit_conf) is 30. The criteria of GATK Variant Filtration is as follows: --clusterWindowSize 10 --filterExpression "MQ0>4 && ((MQ0/(1.0*DP))>0.1)" --filterName "HARD_TO_VALIDATE" --filterExpression "DP<5" --filterName "LowCoverage" --filterExpression "QUAL<30" --filterName "VeryLowQual" --filterExpression "QUAL>30 && QUAL<50" --filterName "LowQual" --filterExpression "QD<1.5" --filterName "LowQD" --filterExpression "FS>150" --filterName "StrandBias". Potential mouse genomic DNA contaminant reads were detected by alignment to the mouse genome (UCSC mm10) and those containing less than 3 mismatches were removed from further analysis. SNVs were called in each sample separately using SAMtools- v0.1.19[57] and GATK in the exome capture targeted regions. Variants with at least Q50 confidence, phred-scaled quality score more than 40 and coverage higher than 10 were considered as true SNVs. Variants were annotated with ANNOVAR (version 11 Feb, 2013)[58]. Identical

variant calls in intestinal stem cells (passage 5 and higher) when compared to passage 0 pooled samples were used to identify germline SNVs. Sanger sequencing validation was performed using primers designed with Primer3 software version 4.0 (http://frodo.wi.mit.edu/). Extracted genomic DNA was amplified with titanium taq polymerase (Clontech Laboratories, CA, USA) and purified PCR products were sequenced in the forward directions using ABI PRISM BigDye Terminator Cycle Sequencing Ready Reaction kits and an ABI PRISM 3730 Genetic Analyzer (Applied Biosystems, CA, USA). We validated by PCR and Sanger sequencing 13 of 14 non-synonymous mutations called by our sequencing efforts suggesting a false discovery rate of less than 10%. Other quality control parameters are shown in Supplementary Information Table 4.

Extended Data

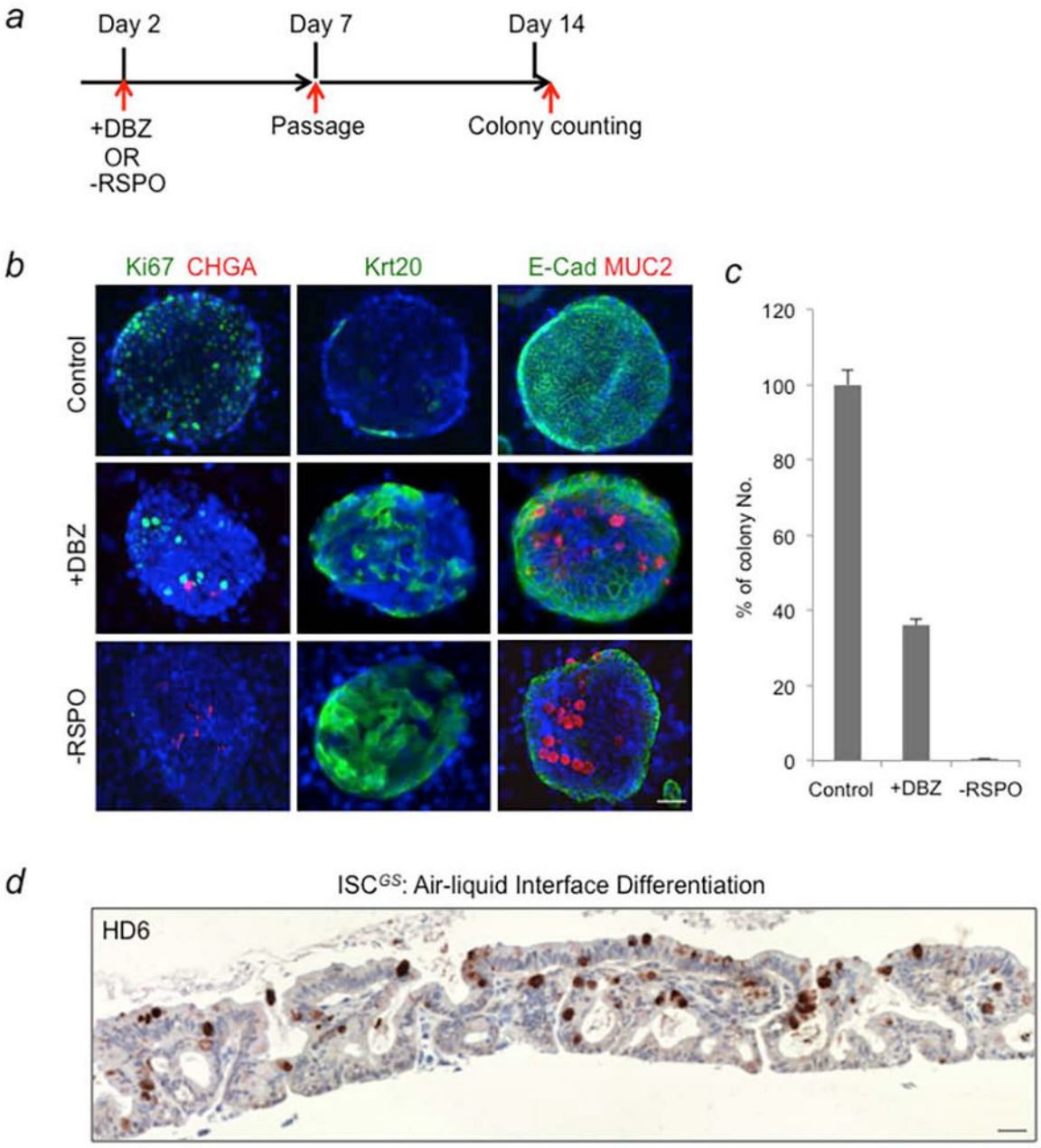

Extended Data Fig. 1. Loss of clonogenicity in differentiated ISC

a. Schematic of ISC differentiation using either the gamma-secretase inhibitor dibenzazepine (DBZ) or withdrawal of the Wnt regulator R-spondin 1 (Rspo1). ISCs were plated on day 0, DBZ added or Rspo1 removed at day 2, and colonies passaged *en mass* at day 7. At day 14, after 7 days of continuous growth, colonies were counted. ***b.*** Micrographs show immunofluorescence at day 7 colonies grown without Rspo1 or in the presence of DBZ for five days using antibodies to Ki67, chromogranin A (CHGA), keratin 20 (Krt20), E-cadherin (E-cad), and mucin 2 (Muc2). Scale bar, 50um; n=4 technical replicates. ***c.***

Histogram shows colony formation in each condition normalized to control ISCs. n=4 biological replicates; Error bars, SD. ***d.*** Staining of ALI-differentiated intestinal stem cells with monoclonal antibody HD6 directed to Paneth cells. Scale bar, 50um; n=4 technical replicates.

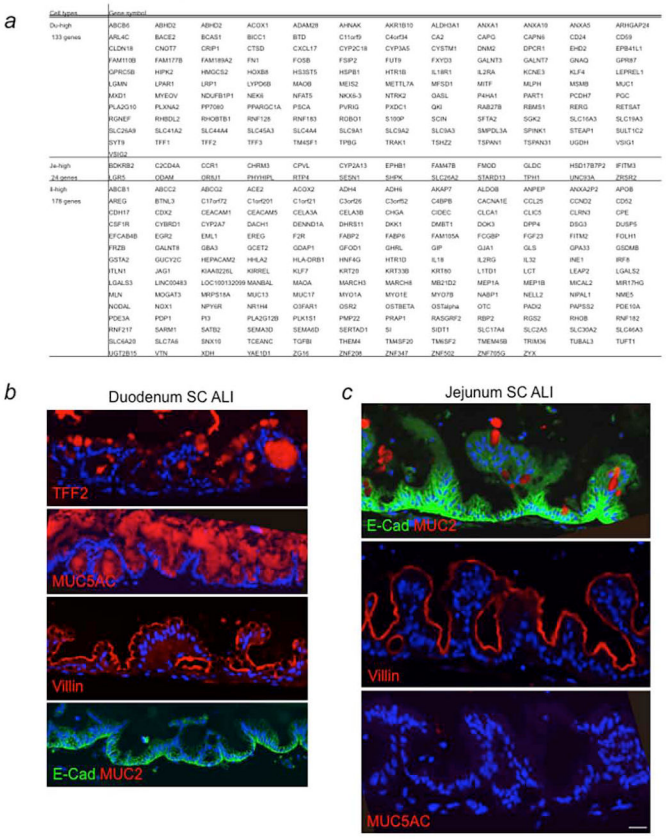

Extended Data Fig. 2. Intestinal stem cell expression profiles

a. List of genes differentially expressed in ISC derived from duodenum, jejunum and ileum. These data correspond to heatmap of Fig. 2b. ***b.*** Immunofluorescence labeling of ALI-differentiated ISCs from duodenum with antibodies against Tff2, mucin 5AC, villin, E-cadherin, and mucin 2. ***c.*** Immunofluorescence labeling of ALI-differentiated epithelia from jejunum stem cells with antibodies to E-cadherin, mucin 2, villin, and mucin 5AC. Scale bar, 50um; n=10 technical replicates.

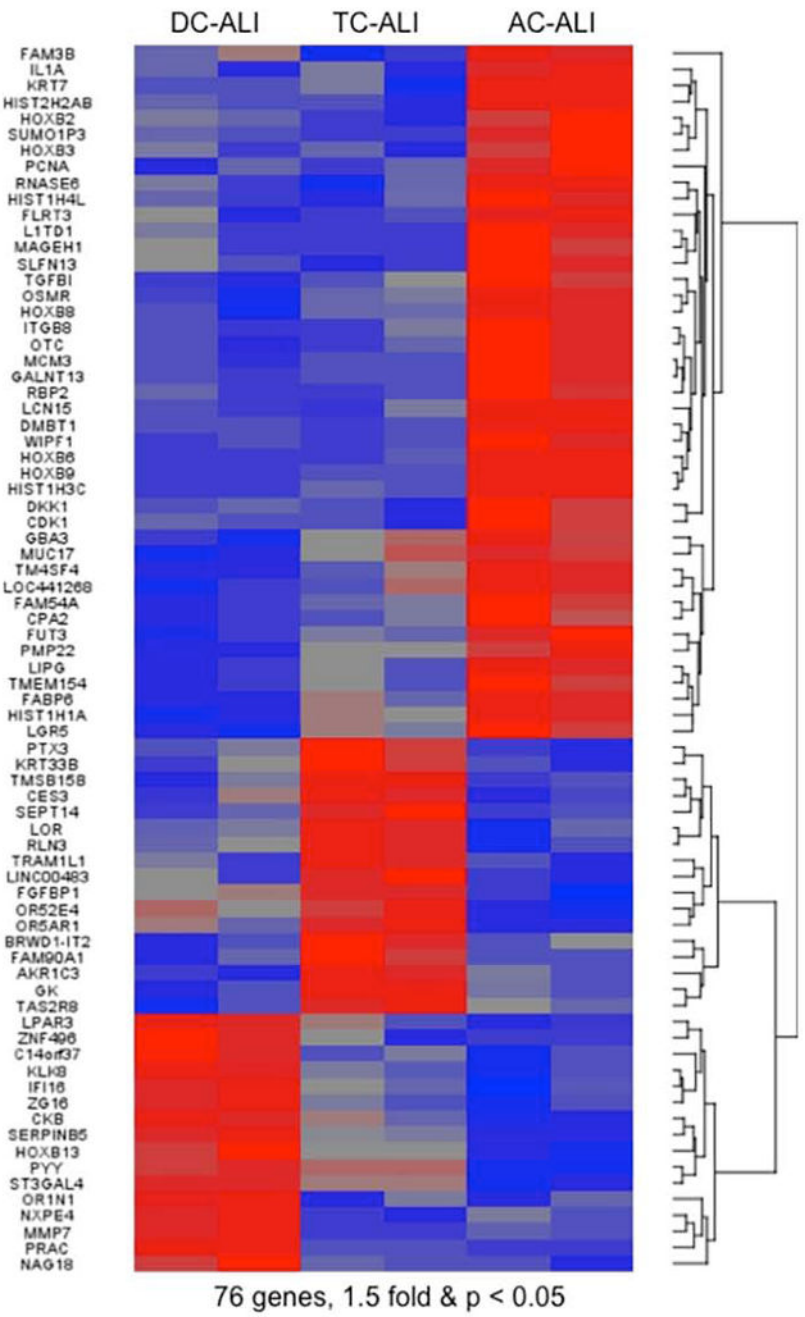

Extended Data Fig. 3. Differential gene expression in epithelia derived from colonic stem cells

Heatmap of differentially expressed (>1.5-fold, p<0.05) genes in ALI cultures derived from stem cell pedigrees of ascending, transverse, and descending colon.

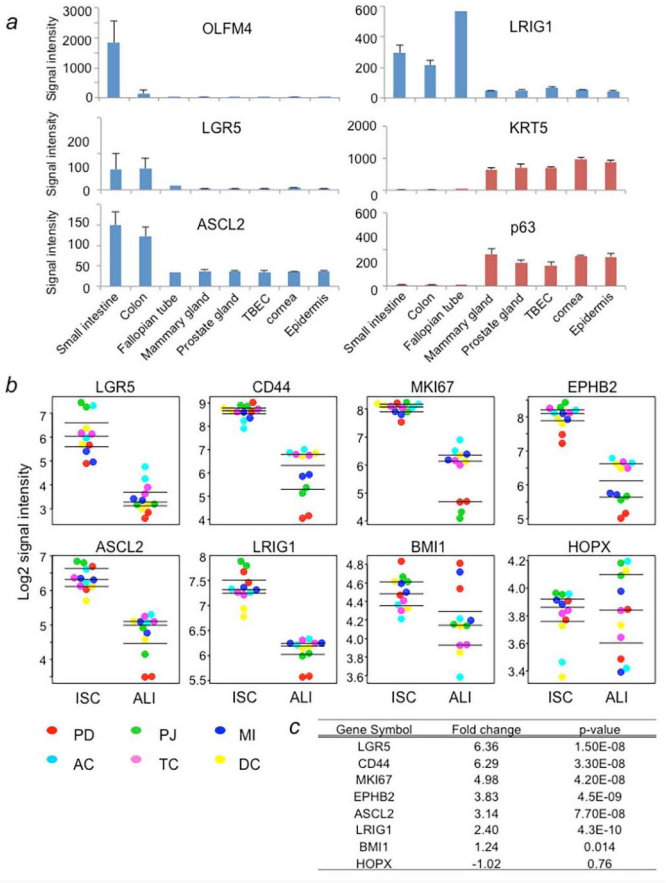

Gene Symbol	Fold change	p-value
LGR5	6.36	1.50E-08
CD44	6.29	3.30E-08
MKI67	4.98	4.20E-08
EPHB2	3.83	4.5E-09
ASCL2	3.14	7.70E-08
LRIG1	2.40	4.3E-10
BMI1	1.24	0.014
HOPX	-1.02	0.76

Extended Data Fig. 4. Differential gene expression across columnar and stratified epithelial stem cells

a. Histograms of expression microarray signal intensity of selected genes across averaged intestine and colon ISCs, stratified epithelial stem cells, and stem cells of the fallopian tube. Biological replicas n=2–6 (FT=2, stratified epithelia=3, colon, intestine=6); Error bars, SD. *b.* Dot plot showing expression microarray data of indicated genes for stem cell pedigrees (ISC; Duo, duodenum; Jej, jejunum; Ile, ileum; AC, ascending colon; TC, transverse colon; DC, descending colon) derived from various regions of the intestinal tract before and after air-liquid interface (ALI) differentiation. Biological replicas n=2 (total 12 datasets) for stem cells, technical replicas n=2 for ALI. *c.* Chart of aggregate p-values by Student t-test for gene expression changes between ground state stem cells and their ALI-differentiated counterparts.

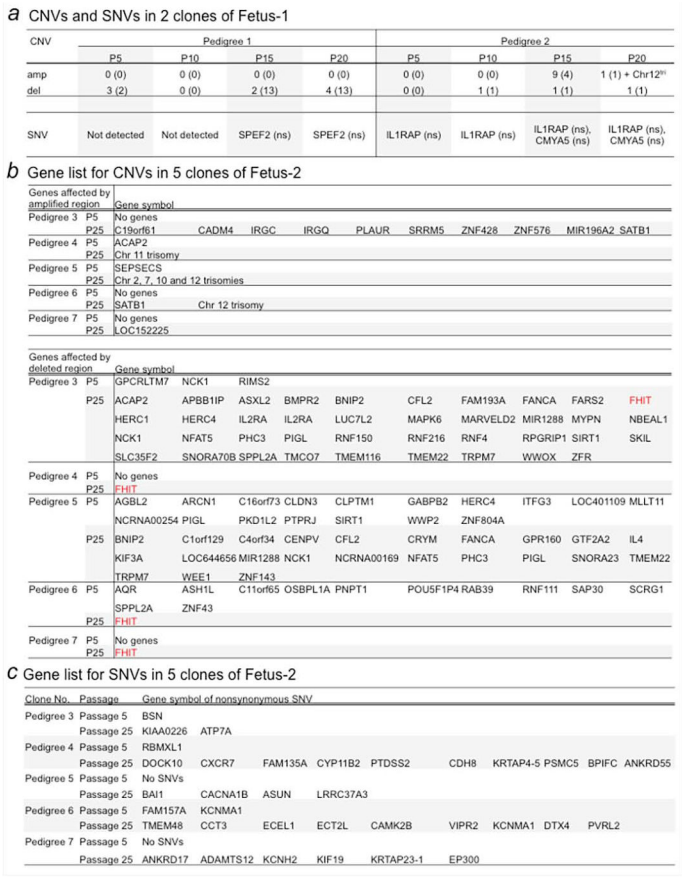

a CNVs and SNVs in 2 clones of Fetus-1

CNV	Pedigree 1				Pedigree 2			
	P5	P10	P15	P20	P5	P10	P15	P20
amp	0 (0)	0 (0)	0 (0)	0 (0)	0 (0)	0 (0)	9 (4)	1 (1) + Chr12[R]
del	3 (2)	0 (0)	2 (13)	4 (13)	0 (0)	1 (1)	1 (1)	1 (1)
SNV	Not detected	Not detected	SPEF2 (ns)	SPEF2 (ns)	IL1RAP (ns)	IL1RAP (ns)	IL1RAP (ns), CMYA5 (ns)	IL1RAP (ns), CMYA5 (ns)

b Gene list for CNVs in 5 clones of Fetus-2

Genes affected by amplified region		Gene symbol									
Pedigree 3	P5	No genes									
	P25	C19orf61	CADM4	IRGC	IRGQ	PLAUR	SRRM5	ZNF428	ZNF576	MIR196A2	SATB1
Pedigree 4	P5	ACAP2									
	P25	Chr 11 trisomy									
Pedigree 5	P5	SEPSECS									
	P25	Chr 2, 7, 10 and 12 trisomies									
Pedigree 6	P5	No genes									
	P25	SATB1	Chr 12 trisomy								
Pedigree 7	P5	No genes									
	P25	LOC152225									

Genes affected by deleted region		Gene symbol									
Pedigree 3	P5	GPCRLTM7	NCK1	RIMS2							
	P25	ACAP2	APBB1IP	ASXL2	BMPR2	BNIP2	CFL2	FAM193A	FANCA	FARS2	FHIT
		HERC1	HERC4	IL2RA	IL2RA	LUC7L2	MAPK6	MARVELD2	MIR1288	MYPN	NBEAL1
		NCK1	NFAT5	PHC3	PIGL	RNF150	RNF216	RNF4	RPGRIP1	SIRT1	SKIL
		SLC35F2	SNORA70B	SPPL2A	TMCO7	TMEM116	TMEM22	TRPM7	WWOX	ZFR	
Pedigree 4	P5	No genes									
	P25	FHIT									
Pedigree 5	P5	AGBL2	ARCN1	C16orf73	CLDN3	CLPTM1	GABPB2	HERC4	ITFG3	LOC401109	MLLT11
		NCRNA00254	PIGL	PKD1L2	PTPRJ	SIRT1	WWP2	ZNF804A			
	P25	BNIP2	C1orf129	C4orf34	CENPV	CFL2	CRYM	FANCA	GPR160	GTF2A2	IL4
		KIF3A	LOC644656	MIR1288	NCK1	NCRNA00169	NFAT5	PHC3	PIGL	SNORA23	TMEM22
		TRPM7	WEE1	ZNF143							
Pedigree 6	P5	AQR	ASH1L	C11orf65	OSBPL1A	PNPT1	POU5F1P4	RAB39	RNF111	SAP30	SCRG1
		SPPL2A	ZNF43								
	P25	FHIT									
Pedigree 7	P5	No genes									
	P25	FHIT									

c Gene list for SNVs in 5 clones of Fetus-2

Clone No.	Passage	Gene symbol of nonsynonymous SNV								
Pedigree 3	Passage 5	BSN								
	Passage 25	KIAA0226	ATP7A							
Pedigree 4	Passage 5	RBMXL1								
	Passage 25	DOCK10	CXCR7	FAM135A	CYP11B2	PTDSS2	CDH8	KRTAP4-5	PSMC5	BPIFC	ANKRD55
Pedigree 5	Passage 5	No SNVs								
	Passage 25	BAI1	CACNA1B	ASUN	LRRC37A3					
Pedigree 6	Passage 5	FAM157A	KCNMA1							
	Passage 25	TMEM48	CCT3	ECEL1	ECT2L	CAMK2B	VIPR2	KCNMA1	DTX4	PVRL2	
Pedigree 7	Passage 5	No SNVs								
	Passage 25	ANKRD17	ADAMTS12	KCNH2	KIF19	KRTAP23-1	EP300			

Extended Data Fig. 5. Genes impacted by CNV and SNV events in intestinal stem cell pedigrees during passaging

a. Summary of CNV [events (genes affected)] and non-synonymous SNV in pedigrees 1 and 2 at P5 to P20. ***b.*** Summary of genes altered by interstitial CNV amplifications (top) or deletions (bottom) in ISC pedigrees no. 3 to 7 at P5 and P25. ***c.*** Summary of genes sustaining non-synonymous SNV in five ISC pedigrees at P5 and P25.

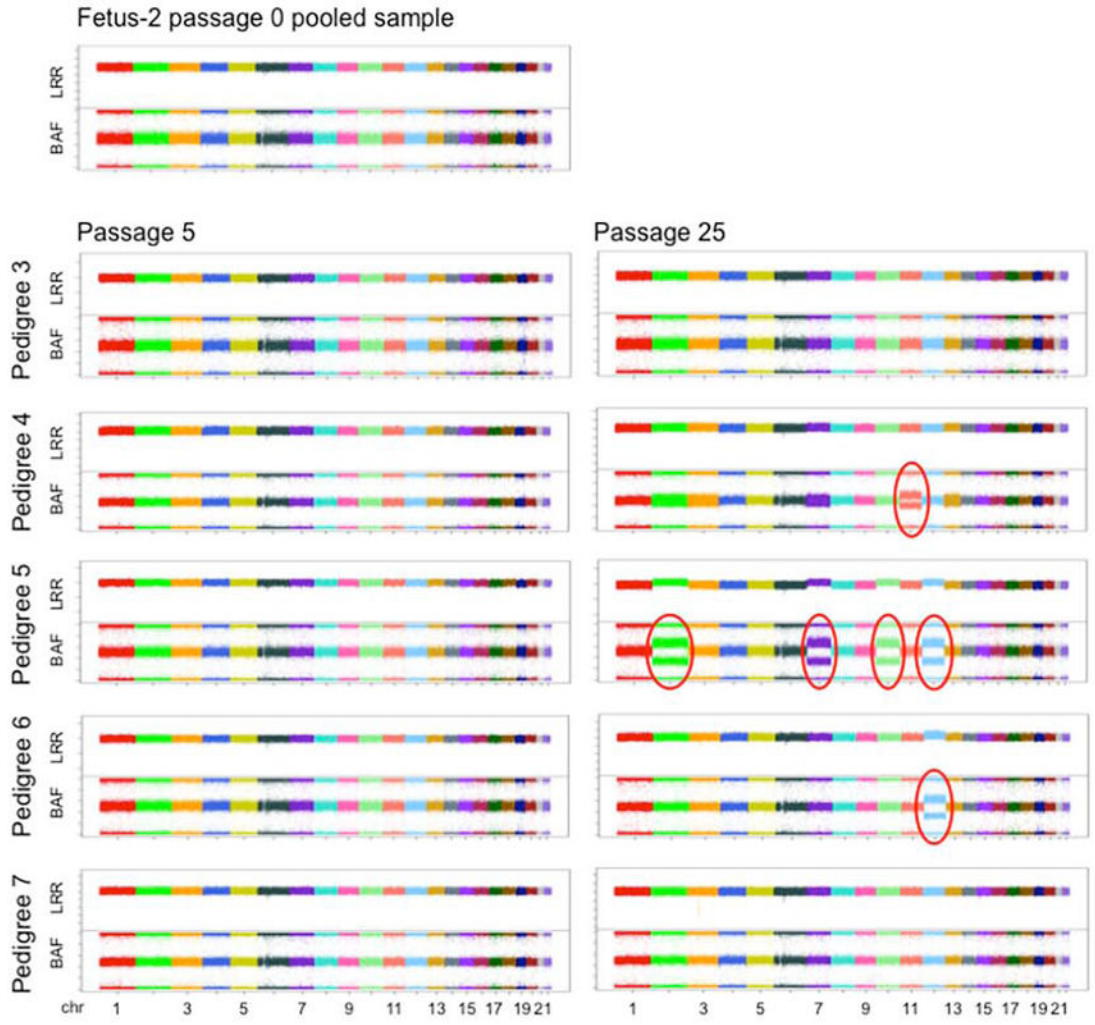

Extended Data Fig. 6.

Whole genome CNV profiles for intestinal stem cell pedigrees 3–7 at P5 and P25. Regions marked by ovals represent aneuploidy.

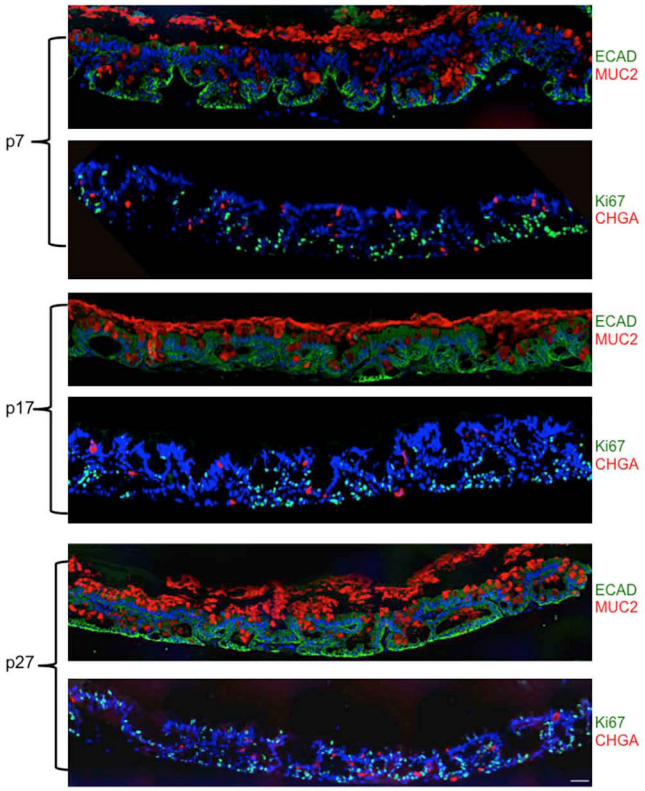

Extended Data Fig. 7. Impact of ISC^{GS} passaging on ALI differentiation

ALI differentiation of intestinal pedigree 2 initiated from cells at the indicated passage number. As indicated, histological sections of differentiated epithelia were stained with antibodies to either E-cadherin (ECAD, green) and mucin 2 (Muc2, red), or Ki67 (green) and chromogranin A (CHGA, red). Scale bar, 75um; n=4 technical replicates.

a

Time / Name	4 wks	8 wks	12 wks	16 wks
Pedigree 3 P6	0/2	0/2	0/2	0/2
Pedigree 3 P25	0/2	0/2	0/2	0/2
Pedigree 5 P6	0/2	0/2	0/2	0/2
Pedigree 5 P25	0/2	0/2	0/2	0/2
Pedigree 7 P6	0/2	0/2	0/2	0/2
Pool	0/2	0/2	0/2	0/2
Cancer Cells	0/8	2/8	5/8	8/8

b

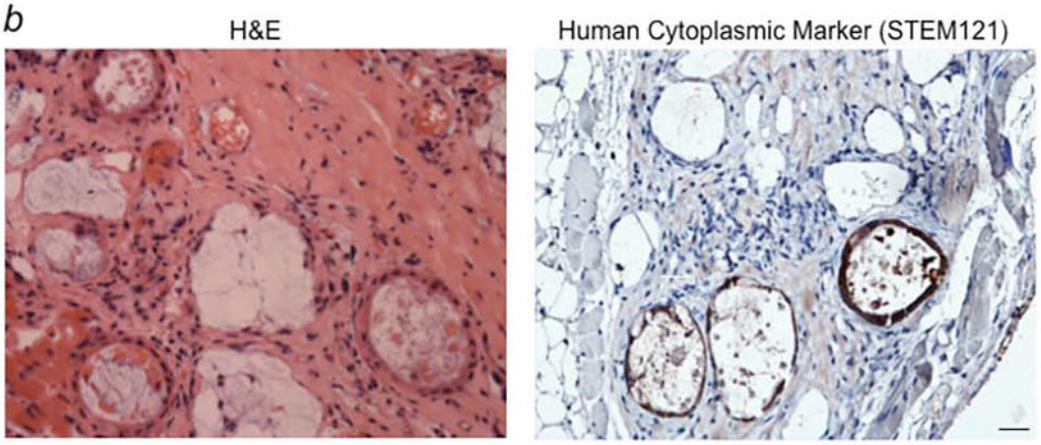

Extended Data Fig. 8. ISC^{GS} tumorigenicity assays in immunodeficient mice

a. Quantification of tumor formation assesses at 4–16 weeks following subcutaneous innoculation of two million cells of the indicated ISC pedigrees at passage 6 or passage 25 at 4–16 weeks. “Pool” indicates total set of clones derived from P0 ileum culture prior to pedigree generation. “Cancer cells” refers to propagating cells from case of high-grade serous ovarian cancer. **b.** *Left*, Histological section through site of injection of 1 million cells from pedigree 3. ***Right,*** Section of injection site stained with antibody (STEM121) to human epithelial cells (brown) revealing benign cysts. Scale bar, 15um.

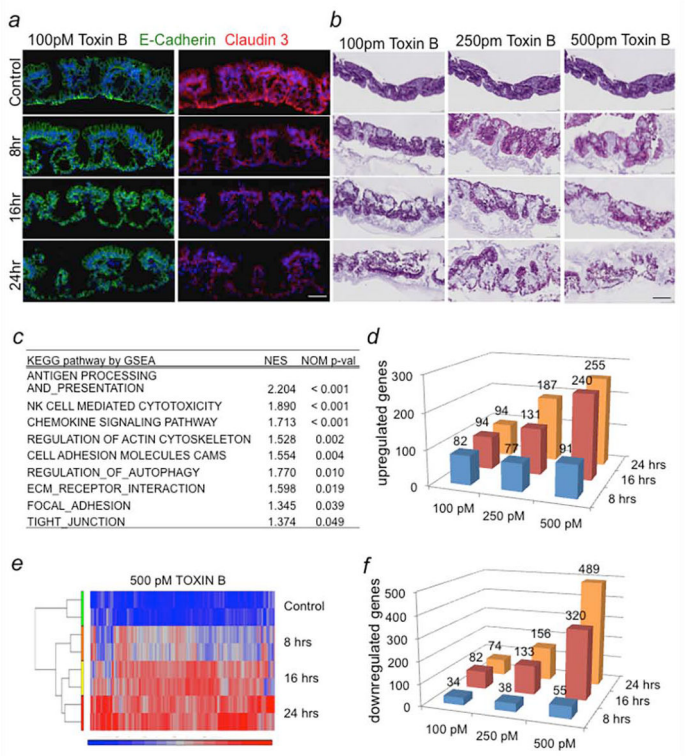

Extended Data Fig. 9. Dose- and time-dependency of TcdB pathology in ALI-generated colonic epithelia

a. Immunofluorescence localization of adherens junction marker E-cadherin and tight junction marker claudin 3 in ALI differentiated epithelia derived from transverse colon stem cells following exposure to 100pM TcdB for the indicated durations. n=4 technical replicates. Scale bar, 100um. ***b.*** Representative H&E images of ALI cultures at indicated times and concentration of TcdB exposure. Scale bar, 250um; n=4 technical replicates. ***c.*** Gene Set Enrichment Analysis of whole genome expression data from colonic epithelia treated with 500pM TcdB for 24 hrs. and control samples showing enriched KEGG pathway sets. NES: normalized enrichment score; NOM p-value: nominal p-value. ***d.*** 3D plot of up-regulated genes at the indicated time points and dosages >2-fold, $p<0.05$). n=2 technical replicates. ***e.*** Heatmap of up-regulated genes in 500 pM TcdB samples. The genes (237 genes) were chosen by cutoff values (>2-fold, $p < 0.05$). Three time points (8, 16 and 24 hrs) are shown. ***f***. 3D plot of down-regulated genes at the indicated time points and dosages >2-fold, $p<0.05$). n=2 technical replicates.

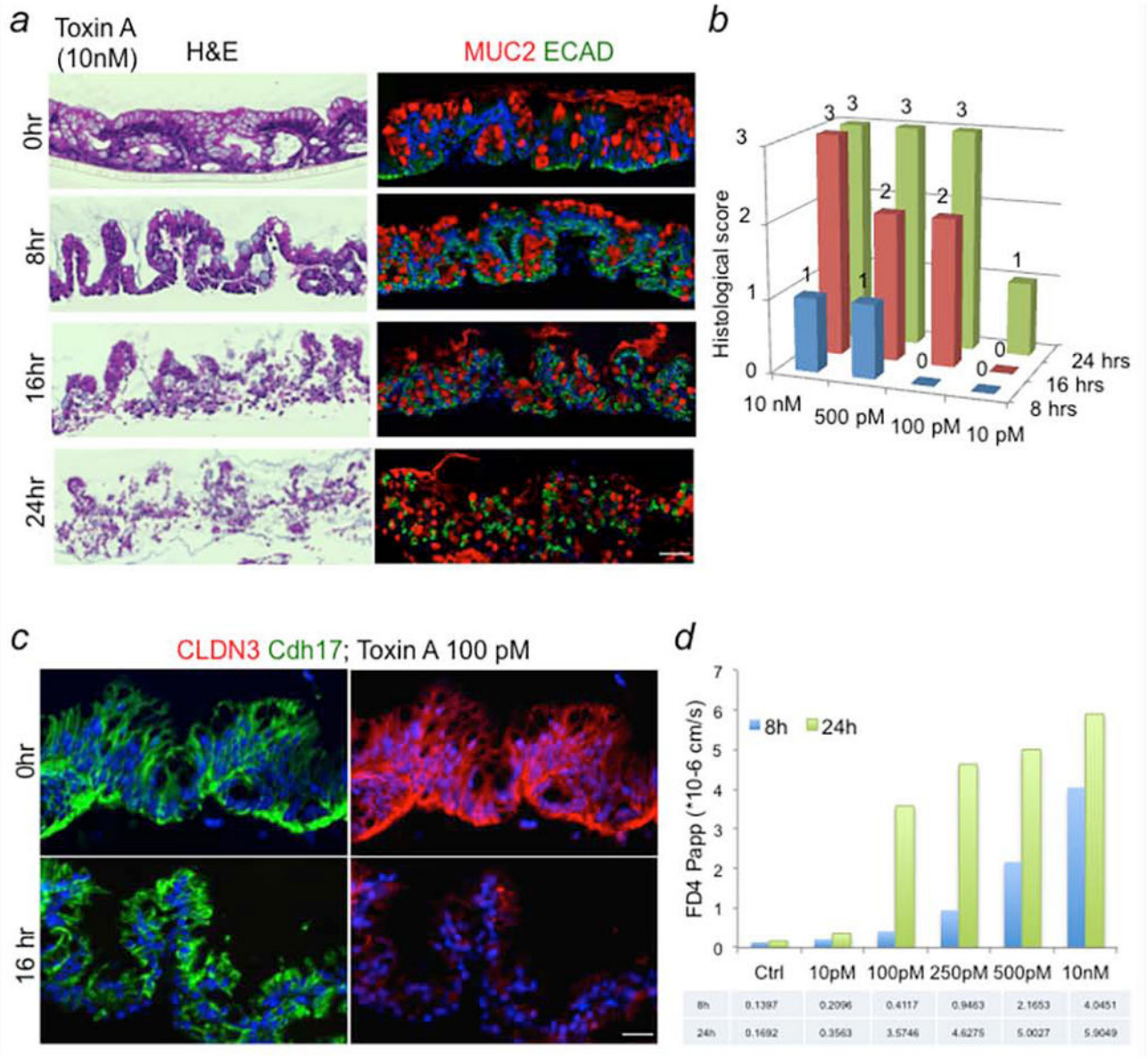

Extended Data Fig. 10. Dose- and time-dependency of TcdA pathology in ALI-generated colonic epithelia

a. left, Representative H&E images of ALI cultures at indicated times and concentration of TcdA exposure; ***right***, Immunofluorescence localization of adherens junction marker E-cadherin (ECAD; green) and mucin 2 (MUC2; red) in ALI differentiated epithelia derived from transverse colon stem cells following incubation with 10nM TcdA for the indicated durations. Scale bar, 100um; n=4 technical replicates. ***b.*** 3-D plot of histological scoring of representative H&E time points and concentrations performed by gastrointestinal pathologist according to a standard 0–3 rating for colonic epithelial integrity. ***c***. Distribution of tight junction marker claudin 3 (Cldn3) and adherens junction marker (Cdh17) following treatment of ALI colonic epithelium with TcdA for the indicated times and doses. Scale bar, 50um; n=4 technical replicates. ***d.*** Histogram of permeability of ALI colonic epithelium

(Papp) to small molecules (FD4, MW 4400Da) following exposure to the indicated doses of TcdA for the indicated times.

Supplementary Material

Refer to Web version on PubMed Central for supplementary material.

Acknowledgments

This work was supported by grants from Connecticut Innovations (WX, FM), the Joint Council Office of the Agency for Science Technology Research Agency (ASTAR), Singapore (WX, FM), the National Medical Research Council, Singapore (BNB101677A to HKY, FM, and WX; BnB11dec063 to NN, FM and WX), the Department of Defense (W81XWH-10-1-0289 to CC) and the National Institute of Health (AI09575504 to DBL). We thank M. LaLande, B. Lane and Benjamin Seet for support, B. Tennent, B. Knowles and T. McLaughlin for comments on the manuscript, J. Hammer for artwork, L. Lapierre and J. Franklin for histology evalutation. We thank H. Green for advice and support.

References

1. Tabar V, Studer L. Pluripotent stem cells in regenerative medicine: challenges and recent progress. Nat Rev Genet. 2014; 15:82–92. [PubMed: 24434846]
2. Okano H, Yamanaka S. iPS cell technologies: significance and applications to CNS regeneration and disease. Mol Brain. 2014; 7:22. [PubMed: 24685317]
3. Müller AM, Dzierzak EA. ES cells have only a limited lymphopoietic potential after adoptive transfer into mouse recipients. Development. 1993; 118:1343–51. [PubMed: 8269860]
4. Helgason CD, Sauvageau G, Lawrence HJ, Largman C, Humphries RK. Overexpression of HOXB4 enhances the hematopoietic potential of embryonic stem cells differentiated in vitro. Blood. 1996; 87:2740–9. [PubMed: 8639890]
5. Bonde S, Dowden AM, Chan KM, Tabayoyong WB, Zavazava N. HOXB4 but not BMP4 confers self-renewal properties to ES-derived hematopoietic progenitor cells. Transplantation. 2008; 86:1803–9. [PubMed: 19104426]
6. Iuchi S, Dabelsteen S, Easley K, Rheinwald JG, Green H. Immortalized keratinocyte lines derived from human embryonic stem cells. Proc Natl Acad Sci U S A. 2006; 103:1792–7. [PubMed: 16446420]
7. Amabile G, Welner RS, Nombela-Arrieta C, D'Alise AM, Di Ruscio A, Ebralidze AK, et al. In vivo generation of transplantable human hematopoietic cells from induced pluripotent stem cells. Blood. 2013; 121:1255–64. [PubMed: 23212524]
8. Suzuki N, Yamazaki S, Yamaguchi T, Okabe M, Masaki H, Takaki S, et al. Generation of engraftable hematopoietic stem cells from induced pluripotent stem cells by way of teratoma formation. Mol Ther. 2013; 21:1424–31. [PubMed: 23670574]
9. Rheinwald JG, Green H. Serial cultivation of strains of human epidermal keratinocytes: the formation of keratinizing colonies from single cells. Cell. 1975; 6:331–43. [PubMed: 1052771]
10. Rama P, Matuska S, Paganoni G, Spinelli A, De Luca M, Pellegrini G. Limbal stem-cell therapy and long-term corneal regeneration. N Engl J Med. 2010; 363:147–155. [PubMed: 20573916]
11. Senoo M, Pinto F, Crum CP, McKeon F. p63 is essential for the proliferative potential of stem cells of stratified epithelia. Cell. 2007; 129:523–536. [PubMed: 17482546]
12. Kumar PA, Hu Y, Yamamoto Y, Hoe NB, Wei TS, Mu D, et al. Distal airway stem cells yield alveoli in vitro and during lung regeneration following H1N1 influenza infection. Cell. 2011; 147:525–538. [PubMed: 22036562]
13. Matsuura R, Kogo H, Ogaeri T, Miwa T, Kuwahara M, Kanai Y, et al. Crucial transcription factors in endoderm and embryonic gut development are expressed in gut-like structures from mouse ES cells. Stem Cells. 2006; 24:624–630. [PubMed: 16210401]

14. Sato T, Vries RG, Snippert HJ, van de Wetering M, Barker N, Stange DE, et al. Single Lgr5 stem cells build crypt-villus structures in vitro without a mesenchymal niche. Nature. 2009; 459:262–5. [PubMed: 19329995]
15. Ootani A, Li X, Sangiorgi E, Ho QT, Ueno H, Toda S, et al. Sustained in vitro intestinal epithelial culture within a Wnt-dependent stem cell niche. Nat Med. 2009; 15:701–706. [PubMed: 19398967]
16. Sato T, van Es JH, Snippert HJ, Stange DE, Vries RG, van den Born M, Barker N, Shroyer NF, van de Wetering M, Clevers H. Paneth cells constitute the niche for Lgr5 stem cells in intestinal crypts. Nature. 2011; 469:415–418. [PubMed: 21113151]
17. Fordham RP, Yui S, Hannan NR, Soendergaard C, Madgwick A, Schweiger PJ, et al. Transplantation of expanded fetal intestinal progenitors contributes to colon regeneration after injury. Cell Stem Cell. 2013; 13:734–744. [PubMed: 24139758]
18. Middendorp S, Schneeberger K, Wiegerinck CL, Mokry M, Akkerman RD, van Wijngaarden S, et al. Adult stem cells in the small intestine are intrinsically programmed with their location-specific function. Stem Cells. 2014; 32:1083–1091. [PubMed: 24496776]
19. Yin X, Farin HF, van Es JH, Clevers H, Langer R, Karp JM. Niche-independent high-purity cultures of Lgr5+ intestinal stem cells and their progeny. Nat Methods. 2014; 11:106–112. [PubMed: 24292484]
20. Kim KA, Kakitani M, Zhao J, Oshima T, Tang T, Binnerts M, et al. Mitogenic influence of human R-spondin1 on the intestinal epithelium. Science. 2005; 309:1256–1259. [PubMed: 16109882]
21. Dreesen O, Brivanlou AH. Signaling pathways in cancer and embryonic stem cells. Stem Cell Rev. 2007; 3:7–17. [PubMed: 17873377]
22. Zhu L, Gibson P, Currle DS, Tong Y, Richardson RJ, Bayazitov IT, et al. Prominin 1 marks intestinal stem cells that are susceptible to neoplastic transformation. Nature. 2009; 457:603–607. [PubMed: 19092805]
23. Barker N, van Es JH, Kuipers J, Kujala P, van den Born M, et al. Identification of stem cells in small intestine and colon by marker gene Lgr5. Nature. 2007; 449:1003–1007. [PubMed: 17934449]
24. Powell AE, et al. The pan-ErbB negative regulator Lrig1 is an intestinal stem cell marker that functions as a tumor suppressor. Cell. 2012; 149:146–158. [PubMed: 22464327]
25. Botrugno OA, Fayard E, Annicotte JS, Haby C, Brennan T, Wendling O, et al. Synergy between LRH-1 and beta-catenin induces G1 cyclin-mediated cell proliferation. Mol Cell. 2004; 15:499–509. [PubMed: 15327767]
26. Lessard J, Sauvageau G. Bmi-1 determines the proliferative capacity of normal and leukaemic stem cells. Nature. 2003; 423:255–60. [PubMed: 12714970]
27. Sangiorgi E, Capecchi MR. Bmi1 is expressed in vivo in intestinal stem cells. Nat Genet. 2008; 40:915–20. [PubMed: 18536716]
28. Tian H, Biehs B, Warming S, Leong KG, Rangell L, Klein OD, de Sauvage FJ. A reserve stem cell population in small intestine renders Lgr5-positive cells dispensable. Nature. 2011; 478:255–259. [PubMed: 21927002]
29. Metcalfe C, Kljavin NM, Ybarra R, de Sauvage FJ. Lgr5+ stem cells are indispensable for radiation-induced intestinal regeneration. Cell Stem Cell. 2014; 14:149–59. [PubMed: 24332836]
30. Battle MA, Bondow BJ, Iverson MA, Adams SJ, Jandacek RJ, Tso P, Duncan SA. GATA4 is essential for jejunal function in mice. Gastroenterology. 2008; 135:1676–1686. [PubMed: 18812176]
31. Walker EM, Thompson CA, Battle MA. GATA4 and GATA6 regulate intestinal epithelial cytodifferentiation during development. Dev Biol. 2014; 392:283–294. [PubMed: 24929016]
32. Dusing MR, Maier EA, Aronow BJ, Wiginton DA. Onecut-2 knockout mice fail to thrive during early postnatal period and have altered patterns of gene expression in small intestine. Physiol Genomics. 2010; 42:115–25. [PubMed: 20354101]
33. Amps K, Andrews PW, Anyfantis G, Armstrong L, Avery S, et al. International Stem Cell Initiative. Screening ethnically diverse human embryonic stem cells identifies a chromosome 20 minimal amplicon conferring growth advantage. Nat Biotechnol. 2011; 29:1132–44. [PubMed: 22119741]

34. Avery S, Hirst AJ, Baker D, Lim CY, Alagaratnam S, Skotheim RI, et al. BCL-XL Mediates the Strong Selective Advantage of a 20q11.21 Amplification Commonly Found in Human Embryonic Stem Cell Cultures. Stem Cell Reports. 2013; 1:379–86. [PubMed: 24286026]
35. Shultz LD, Goodwin N, Ishikawa F, Hosur V, Lyons BL, Greiner DL. Human cancer growth and therapy in immunodeficient mouse models. Cold Spring Harb Protoc. 2014; 2014:694–708. [PubMed: 24987146]
36. Voth DE, Ballard JD. Clostridium difficile toxins: mechanism of action and role in disease. Clin Microbiol Rev. 2005; 18:247–263. [PubMed: 15831824]
37. Carter GP, Rood JI, Lyras D. The role of toxin A and toxin B in the virulence of Clostridium difficile. Trends Microbiol. 2012; 20:21–9. [PubMed: 22154163]
38. Lyras D, O'Connor JR, Howarth PM, Sambol SP, Carter GP, Phumoonna T, Poon R, Adams V, Vedantam G, Johnson S, Gerding DN, Rood JI. Toxin B is essential for virulence of Clostridium difficile. Nature. 2009; 458:1176–1179. [PubMed: 19252482]
39. Farrow MA, Chumbler NM, Lapierre LA, Franklin JL, Rutherford SA, Goldenring JR, Lacy DB. Clostridium difficile toxin B-induced necrosis is mediated by the host epithelial cell NADPH oxidase complex. Proc Natl Acad Sci U S A. 2013; 110:18674–18679. [PubMed: 24167244]
40. Huelsenbeck J, Dreger SC, Gerhard R, Fritz G, Just I, Genth H. Upregulation of the immediate early gene product RhoB by exoenzyme C3 from Clostridium limosum and toxin B from Clostridium difficile. Biochemistry. 2007; 46:4923–4931. [PubMed: 17397186]
41. Aktories K, Schmidt G, Just I. Rho GTPases as targets of bacterial protein toxins. Biol Chem. 2000; 381:421–426. [PubMed: 10937872]
42. MacFie TS, Poulsom R, Parker A, Warnes G, Boitsova T, Nijhuis A, Suraweera N, Poehlmann A, Szary J, Feakins R, Jeffery R, Harper RW, Jubb AM, Lindsay JO, Silver A. DUOX2 and DUOXA2 form the predominant enzyme system capable of producing the reactive oxygen species H2O2 in active ulcerative colitis and are modulated by 5-aminosalicylic acid. Inflamm Bowel Dis. 2014; 20:514–524. [PubMed: 24492313]
43. Cheng H, Leblond CP. Origin, differentiation and renewal of the four main epithelial cell types in the mouse small intestine. V. Unitarian Theory of the origin of the four epithelial cell types. Am J Anat. 1974; 141:537–561. [PubMed: 4440635]
44. Yui S, Nakamura T, Sato T, Nemoto Y, Mizutani T, Zheng X, et al. Functional engraftment of colon epithelium expanded in vitro from a single adult $Lgr5^{+}$ stem cell. Nat Med. 2012; 18:618–23. [PubMed: 22406745]
45. Wang F, Scoville D, He XC, Mahe MM, Box A, Perry JM, Smith NR, Lei NY, Davies PS, Fuller MK, Haug JS, McClain M, Gracz AD, Ding S, Stelzner M, Dunn JC, Magness ST, Wong MH, Martin MG, Helmrath M, Li L. Isolation and characterization of intestinal stem cells based on surface marker combinations and colony-formation assay. Gastroenterology. 2013; 145:383–395. [PubMed: 23644405]
46. Watson CL, Mahe MM, Múnera J, Howell JC, Sundaram N, Poling HM, Schweitzer JI, Vallance JE, Mayhew CN, Sun Y, Grabowski G, Finkbeiner SR, Spence JR, Shroyer NF, Wells JM, Helmrath MA. An in vivo model of human small intestine using pluripotent stem cells. Nat Med. 2014; 20:1310–1314. [PubMed: 25326803]
47. Sheaffer KL, Kaestner KH. Transcriptional networks in liver and intestinal development. Cold Spring Harb Perspect Biol. 2012; 4:a008284. [PubMed: 22952394]
48. Nicholson JK, Holmes E, Kinross J, Burcelin R, Gibson G, Jia W, Pettersson S. Host-gut microbiota metabolic interactions. Science. 2012; 336:1262–1267. [PubMed: 22674330]
49. Brandl K, Beutler B. Creating diseases to understand what prevents them: genetic analysis of inflammation in the gastrointestinal tract. Curr Opin Immunol. 2012; 24:678–85. [PubMed: 23123276]
50. Lees CW, Barrett JC, Parkes M, Satsangi J. New IBD genetics: common pathways with other diseases. Gut. 2011; 60:1739–1753. [PubMed: 21300624]
51. Schmidt D, Hübsch U, Wurzer H, Heppt W, Aufderheide M. Development of an in vitro human nasal epithelial (HNE) cell model. Toxicol Lett. 1996; 88:75–79. [PubMed: 8920719]
52. Chumbler NM, et al. Clostridium difficile Toxin B causes epithelial cell necrosis through an autoprocessing-independent mechanism. PLoS Pathog. 2012; 8:e1003072. [PubMed: 23236283]

53. Subramanian A, et al. Gene set enrichment analysis: a knowledge-based approach for interpreting genome-wide expression profiles. Proc Natl Acad Sci U S A. 2005; 102:15545–15550. [PubMed: 16199517]

54. Wang K, et al. PennCNV: an integrated hidden Markov model designed for high-resolution copy number variation detection in whole-genome SNP genotyping data. Genome res. 2007; 17:1665–1674. [PubMed: 17921354]

55. Li H, Durbin R. Fast and accurate short read alignment with Burrows-Wheeler Transform. Bioinformatics. 2009; 25:1754–1760. [PubMed: 19451168]

56. McKenna A, et al. The Genome Analysis Toolkit: a MapReduce framework for analyzing next-generation DNA sequencing data. Genome Res. 2010; 20:1297–303. [PubMed: 20644199]

57. Li H, et al. The Sequence Alignment/Map format and SAMtools. Bioinformatics. 2009; 25:2078–2079. [PubMed: 19505943]

58. Wang K, Li M, Hakonarson H. ANNOVAR: functional annotation of genetic variants from high-throughput sequencing data. Nucleic Acids Res. 2010; 38:e164. [PubMed: 20601685]

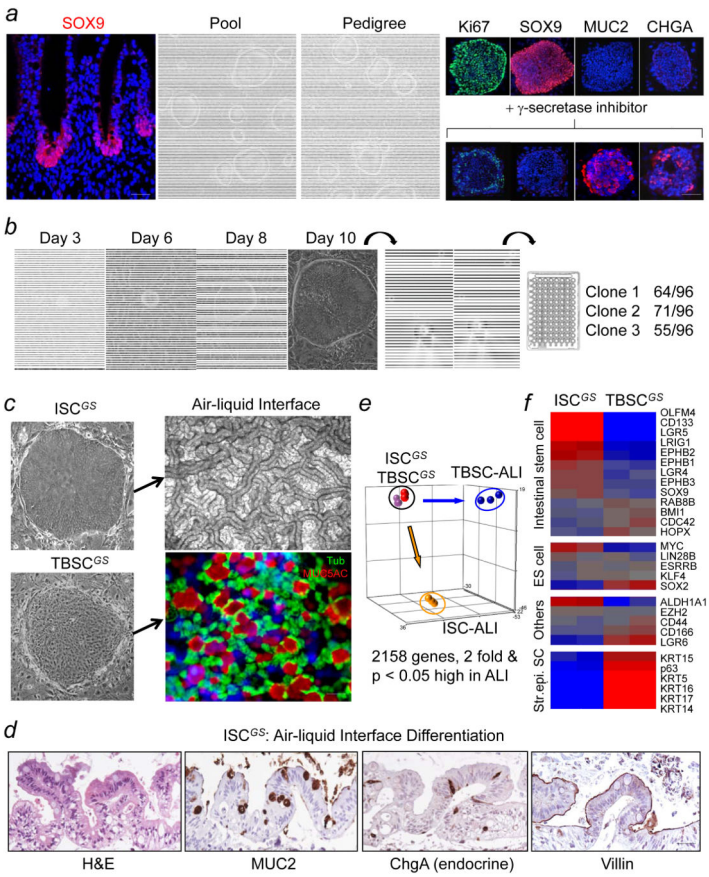

Figure 1. Cloning stem cells from fetal intestine

a. Sox9 expression in fetal intestine, scale bar, 25um; colonies from intestine (n=10 biological replicates; colonies of ISC pedigree (n=30 independent experiments). Scale bar, 75um. *Right*, ISC colonies stained with indicated antibodies. n=4 technical replicates. *Bottom*, Marker expression following Notch inhibition. n=4 technical replicates. ***b.*** ISC colony growth. Scale bar, 75um. *Right*, Clonogenicity of colony cells. n=3 biological replicates. ***c.*** ISC and TBSC pedigrees and ALI differentiation (tubulin, green; Muc5AC, red). Scale bar, 50um left, 25um right top, 25um bottom right; n=7 biological replicates; n=3 technical replicates; 3 independent experiments ***d.*** ALI-differentiated ISC. Scale bar, 50um. n=7 biological replicates; n=3 technical replicates; 3 independent experiments. ***e.*** PCA using 2158 genes (>2-fold, p<0.05 by Student t-Test) of ISC and TBSC and corresponding ALI-differentiated epithelia. ***f.*** Markers in ISC and TBSC. n=3 technical replicates.

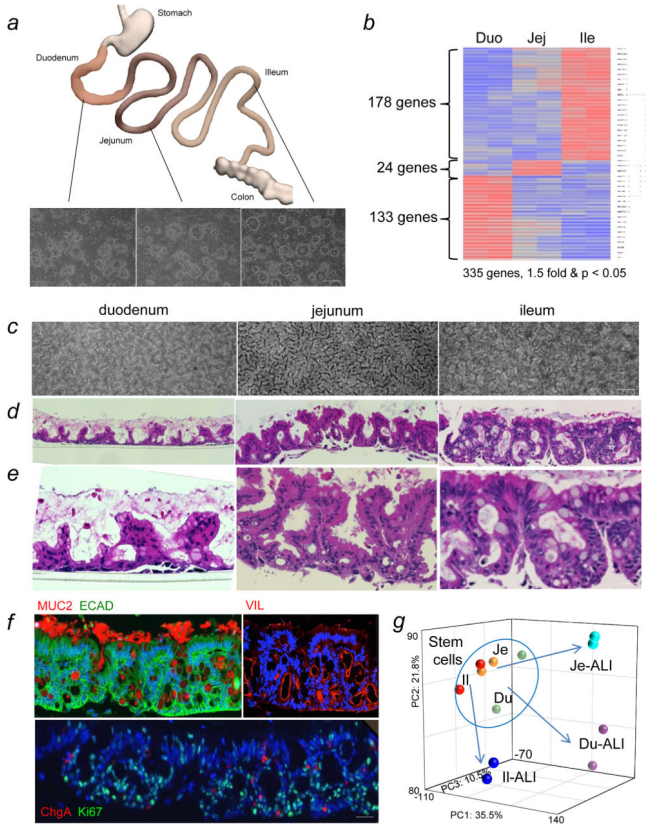

Figure 2. Stem cells from fetal small intestine

a. Depiction of small intestine and clones derived from each. Scale bar, 400um; n=3 biological replicates. ***b.*** Heatmap of pedigrees from duodenum (Du), jejunum (JE), and ileum (Il). **c.** Surface views of ALI cultures. Scale bar, 200um; n=30 technical replicates. ***d.,e.*** Histological sections through ALI cultures at low (Scale bar, 150um) and high Scale bar, 50um) magnification. ***f.*** Immunofluorescence on sections of ALI cultures with indicated antibodies. Scale bar, 75um; n=3 technical replicates. ***g.*** PCA map of stem cell gene expression from the three major regions of the small intestine together with their corresponding ALI-differentiated epithelia.

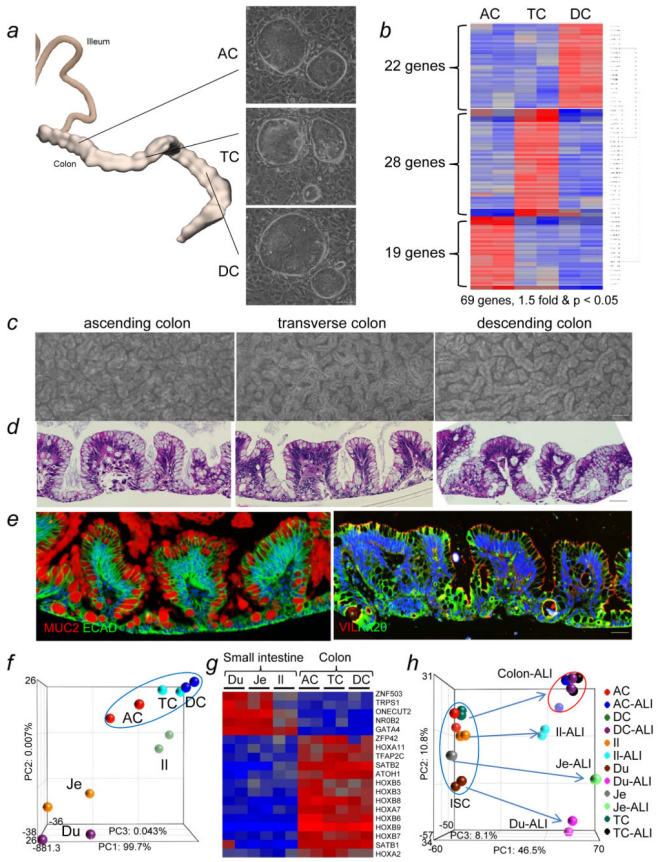

Figure 3. Stem cells of fetal colon

a. Depiction of colon and clones derived from each. Scale bar, 75um; n=3 biological replicates. ***b.*** Expression heatmap of pedigrees from the three major divisions of the colon. ***c.*** Surface images of ALI cultures. Scale bar, 100um; n=20 technical replicates. ***d.*** Histological sections through ALI cultures of colon stem cells. Scale bar, 75um. ***e.*** Immunofluorescence on sections through ALI cultures with indicated antibodies. Scale bar, 50um. ***f.*** PCA map of gene expression of colon and intestine stem cells. ***g.*** Expression heatmap of stem cells of small intestine and colon. ***h.*** PCA map of gene expression profiles of intestinal stem cells and their corresponding ALI-differentiated epithelia.

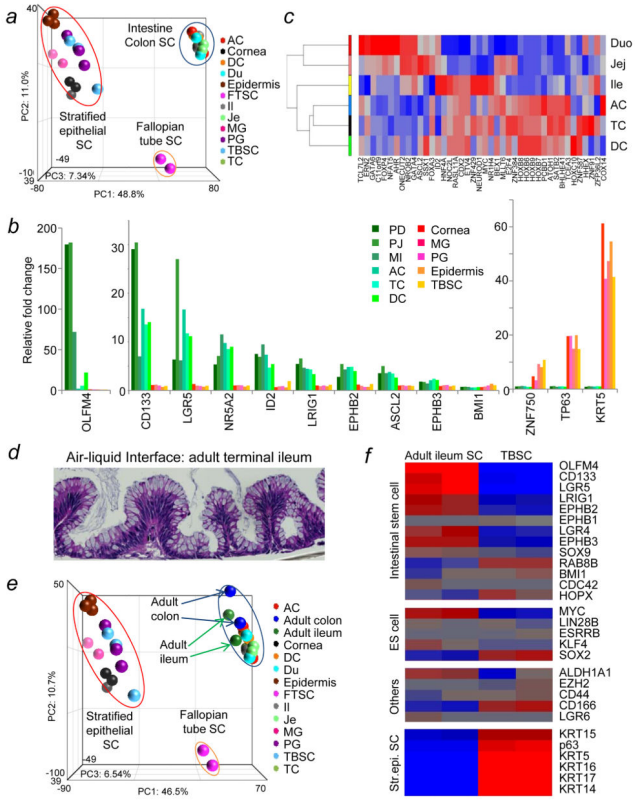

Figure 4. Differential gene expression in stem cells of stratified and columnar epithelia

a. PCA map of stem cells of stratified epithelia (corneal epithelium, *Cor*; mammary gland, *MG*; prostate gland, *PG*; epidermis, *Epi*; tracheobronchial epithelium; *TB*) and columnar epithelia (fallopian tube epithelium, *FTSC*). ***b.*** Gene expression in stem cells (stratified epithelia n=3 technical replicates; columnar epithelia n=2 technical replicates). ***c.*** Transcription factors differentially expressed in TBSC and ISC. ***d.*** ALI differentiated adult terminal ileum stem cells derived from endoscopic biopsy. Scale bar, 50um; n=10 technical replicates. ***e.*** PCA map of stem cells of adult terminal ileum, colon, fetal ISCs, and stratified epithelia. ***f.*** Stem cell markers in adult terminal ileum stem cells and TBSCs.

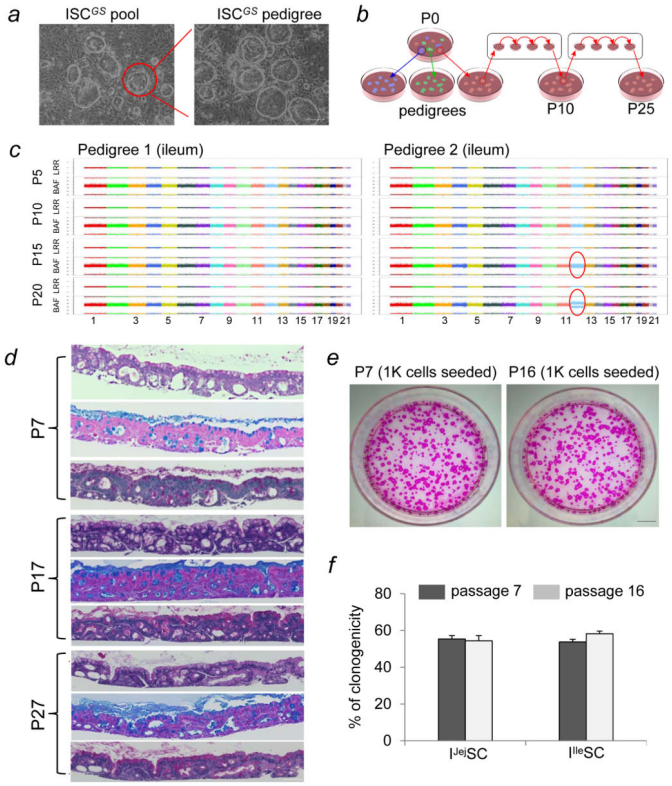

Figure 5. Genomic stability of ISC in culture

a. Clone selection for pedigree generation. Scale bar, 200um. ***b.*** Serial passaging of pedigrees. ***c.*** CNV BAF and LRR profiles of pedigrees at P5 to P20 and trisomy 12 indicated (circle). ***d.*** ALI-differentiated pedigree 2 at P7, 17, and P27 stained with H&E (top), Alcian blue (middle), and periodic acid-Schiff (bottom). Scale bar, 100um; n=4 technical replicates. ***e.*** Clonogenicity assay revealing Rhodamine red-stained colonies grown 20 days following seeding 1,000 passaged cells. Scale bar, 10mm; n=3 technical replicates. ***f.*** Quantification of clonogenicity at indicated passage number of ground state stem cells from jejunum ($I^{Jej}SC$) and ileum ($I^{Ile}SC$). n=3 biological replicates; Error, SD.

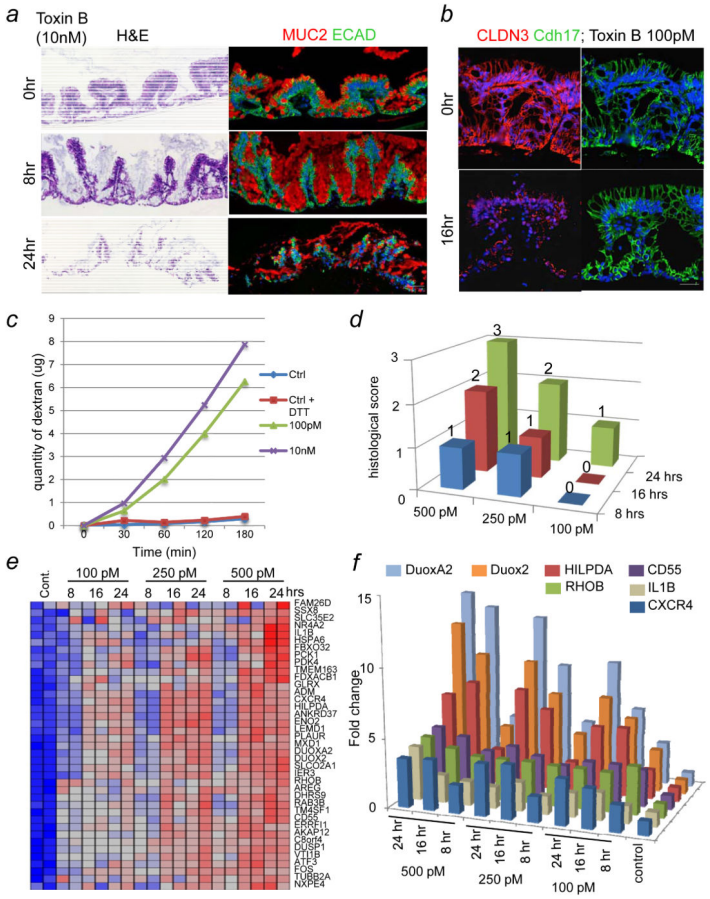

Figure 6. *C. difficile* Toxin B effects on *in vitro* generated colonic epithelia

a. TcdB effects on colonic stem cell-derived epithelia. Scale bar, 100um. n=4 technical replicates. ***b.*** Tight junction protein claudin 3 (CLDN3; red) and adherens junction marker cadherin-17 (CDH17; green) in ALI colonic epithelium TcdB. Scale bar, 50um; n=4 biological replicates. ***c.*** Dextran permeability assay on TcdB-treated ALI colonic epithelia. ***d.*** 3-D plot of histological scoring by gastrointestinal pathologist according to a standard 0–3 rating for colonic epithelial integrity. ***e.*** Heatmap of thirty-nine genes differentially expressed between TcdB (500 pM 24 hrs) and controls (>3-fold and $p < 0.05$ by Student t-Test). ***f.*** 3-D plot of seven selected genes at time points and doses indicated. n=2 technical replicates.